

Black holes in Einstein-Gauß-Bonnet-dilaton theory

Jose Luis Blázquez-Salcedo ¹, Vitor Cardoso ², Valeria Ferrari ³,
 Leonardo Gualtieri ³, Panagiota Kanti ⁴, Fei Chen Khoo ⁵,
 Burkhard Kleihaus ¹, Jutta Kunz ¹, Caio F. B. Macedo ⁶,
 Sindy Mojica ⁷, Paolo Pani ³ and Eugen Radu ⁸

¹Institut für Physik, Universität Oldenburg, Postfach 2503, D-26111 Oldenburg, Germany

²CENTRA, Departamento de Física, Instituto Superior Técnico, Universidade de Lisboa
 Avenida Rovisco Pais 1, 1049 Lisboa, Portugal

³Dipartimento di Fisica, “Sapienza” Università di Roma & Sezione INFN Roma1
 Piazzale Aldo Moro 5, 00185 Roma, Italy

⁴ Division of Theoretical Physics, Department of Physics, University of Ioannina
 Ioannina GR-45110, Greece

⁵Department of Physics and Earth Sciences, Jacobs University, D-28759 Bremen, Germany

⁶Faculdade de Física, Universidade Federal do Pará 66075-110 Belém, Pará, Brazil

⁷Escuela de Física, Universidad Industrial de Santander
 A. A. 678, Bucaramanga 680002, Colombia

⁸Departamento de Física da Universidade de Aveiro and CIDMA
 Campus de Santiago, 3810-183 Aveiro, Portugal

Abstract. Generalizations of the Schwarzschild and Kerr black holes are discussed in an astrophysically viable generalized theory of gravity, which includes higher curvature corrections in the form of the Gauss-Bonnet term, coupled to a dilaton. The angular momentum of these black holes can slightly exceed the Kerr bound. The location and the orbital frequency of particles in their innermost stable circular orbits can deviate significantly from the respective Kerr values. Study of the quasinormal modes of the static black holes gives strong evidence that they are mode stable against polar and axial perturbations. Future gravitational wave observations should improve the current bound on the Gauss-Bonnet coupling constant, based on observations of the low-mass x-ray binary A 0620-00.

Keywords. Relativity, gravitation, black hole physics, gravitational waves

1. Introduction

So far General Relativity (GR) has passed all tests in the Solar System and beyond. Still we expect that GR will be superseded by a generalized theory of gravity, which encompasses GR as a limit. Reasons for this expectation reside on the one hand on the theoretical side, where the incompatibility of GR with quantum mechanics has sparked the search for a theory of quantum gravity. On the other hand, when GR is applied to the evolution of the Universe as a whole, the necessity for the presence of dark matter and dark energy arises, the nature of which is currently unknown.

By now a large number of alternative theories of gravity have been proposed and some of their implications for astrophysical objects have been studied. The review *Testing General Relativity with Present and Future Astrophysical Observations* by Berti *et al.* (2015) gives a broad account of recent activities in this area.

Here we consider Einstein–Gauss-Bonnet-dilaton (EGBd) gravity, which represents a

very interesting and well motivated extension of GR. The EGBd action is obtained by adding a real scalar field, a dilaton, to the GR action which is non-minimally coupled to the Gauss-Bonnet (GB) term. The resulting theory of gravity has quadratic curvature terms, but it has only second order equations of motion. Moreover, the EGBd action arises naturally in the framework of the low-energy effective string theories (see *e.g.* Moura & Schiappa (2007)).

To represent a viable alternative theory of gravity, EGBd theory must satisfy theoretical and observational constraints. These yield bounds on the GB coupling constant α . Solar system measurements, as *e.g.*, measurements of the Shapiro time delay, yield the rather weak bound, $\sqrt{\alpha} \lesssim 10^{13} \text{cm}$ (Bertotti, Iess & Tortora (2003)). In contrast, black holes in low-mass x-ray binaries can give a much stronger bound, since black holes in EGBd theory carry a scalar charge. Observations of the black hole low-mass x-ray binary A0620-00 (Cantrell *et al.* (2010)) then lead to a constraint based on the orbital decay rate (Yagi (2012))

$$\sqrt{\alpha} \lesssim 10^6 \text{cm} . \quad (1.1)$$

From the theoretical side the mere existence of black hole solutions implies an upper bound (Kanti *et al.* (1996), Pani & Cardoso (2009))

$$\frac{\alpha}{M^2} \lesssim 0.691 . \quad (1.2)$$

Future observations of quasi-periodic oscillations (QPOs) from accreting black holes could be used to further constrain the theory (Maselli *et al.* (2015)).

Here we explore the physical properties of static and rotating EGDd black holes (Mignemi & Stewart (1993), Kanti *et al.* (1996), Torii, Yajima & Maeda (1996), Pani & Cardoso (2009), Kleihaus, Kunz & Radu (2011), Pani *et al.* (2011), Ayzenberg & Yunes (2014), Kleihaus, Kunz & Mojica (2014), Maselli *et al.* (2015), Kleihaus *et al.* (2016), Blázquez-Salcedo *et al.* (2016)). In particular, we study their domain of existence and point out their differences to the Schwarzschild and Kerr black holes of GR. By computing the quasinormal modes of the static EGBd black holes, we infer their mode stability. Finally we address how future gravitational wave observations may improve the current bound on the GB coupling constant.

2. Einstein-Gauss-Bonnet-dilaton gravity

The action of EGBd gravity is given by

$$S = \frac{1}{16\pi} \int d^4x \sqrt{-g} \left[R - \frac{1}{2}(\partial_\mu \phi)^2 + \frac{\alpha}{4} e^\phi R_{\text{GB}}^2 \right] , \quad (2.1)$$

where R is the curvature scalar, ϕ is a real scalar field, and α is the GB coupling constant. The dilaton coupling constant has been given its string theory value throughout, and R_{GB}^2 is the Gauss-Bonnet term, which is quadratic in curvature

$$R_{\text{GB}}^2 = R_{\mu\nu\rho\sigma} R^{\mu\nu\rho\sigma} - 4R_{\mu\nu} R^{\mu\nu} + R^2 . \quad (2.2)$$

The resulting set of equations of motion are of second order. The “modified” Einstein equations read

$$G_{\mu\nu} = \frac{1}{2} T_{\mu\nu} \quad (2.3)$$

with the effective stress-energy tensor

$$T_{\mu\nu} = T_{\mu\nu}^{(\phi)} + \frac{\alpha}{2} e^\phi T_{\mu\nu}^{(\text{GBd})} , \quad (2.4)$$

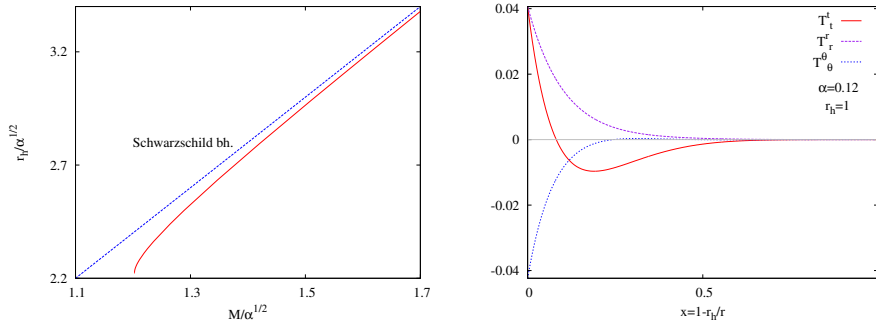


Figure 1. Scaled horizon radius r_h versus scaled mass M of static EGBd black holes with comparison to Schwarzschild black holes (left). Profile of the components of the effective stress-energy tensor, T^t_t , T^r_r and T^θ_θ , for a typical static EGBd black hole (right).

where

$$T_{\mu\nu}^{(\phi)} = \nabla_\mu \phi \nabla_\nu \phi - \frac{1}{2} g_{\mu\nu} \nabla_\lambda \phi \nabla^\lambda \phi \quad (2.5)$$

$$T_{\mu\nu}^{(\text{GBd})} = H_{\mu\nu} + 4 (\nabla^\rho \phi \nabla^\sigma \phi + \nabla^\rho \nabla^\sigma \phi) P_{\mu\rho\nu\sigma} , \quad (2.6)$$

where $H_{\mu\nu}$ is quadratic and $P_{\mu\rho\nu\sigma}$ is linear in the curvature.

The dilaton equation is given by

$$\nabla^2 \phi = \frac{\alpha}{4} e^\phi R_{\text{GB}}^2 . \quad (2.7)$$

Because of the contributions from the GB term on the right hand side of the Einstein equations, the theory allows for negative “effective” energy densities giving rise to black holes with scalar “hair”, although secondary. Moreover, this theory allows for wormholes without the need for exotic matter (Kanti, Kleihaus & Kunz (2012)).

3. Black hole properties

The vacuum black holes in GR consist of the family of static Schwarzschild and rotating Kerr black holes, which in general form the basis of current analyses of astrophysical observations. The GR black holes possess very special properties, in particular, all Kerr black holes are uniquely described by only two parameters, their mass M and their angular momentum J . For Kerr black holes the ratio $j = J/M^2$ is bounded, $|j| \leq 1$, with the extremal black holes saturating the limit.

Static EGBd black holes.

The full set of static EGBd black holes was first constructed by Kanti *et al.* (1996). In this analysis it was realized, that unlike GR black holes the EGBd black holes possess a lower bound for the size and for the mass, when the GB coupling is kept fixed, i.e., for a given theory. This bound arises when the metric and dilaton functions are expanded at the horizon r_h , since the expansion for the dilaton involves a coefficient with a square root

$$\sqrt{1 - 6 \frac{\alpha^2}{r_h^4} e^{2\phi_h}} , \quad (3.1)$$

whose radicand should not be negative in order to retain a real value for the scalar field.

We demonstrate the dependence of the horizon radius r_h on the mass M for the static EGBd black holes in Fig. 1 in the vicinity of the minimal mass and the minimal radius.

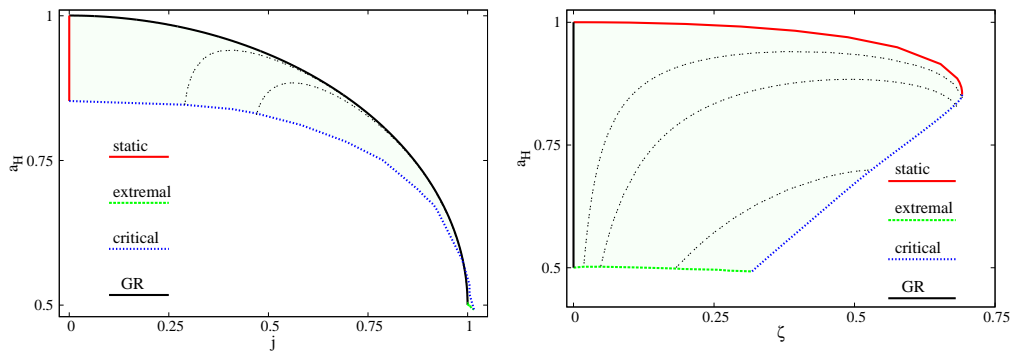


Figure 2. The scaled area versus the scaled angular momentum (left). The scaled area versus the scaled GB coupling constant (right). Also indicated are the static, the extremal, the critical and the GR black holes.

It is the presence of the minimal mass, which leads to the bound (1.2). We also note from the figure, that whereas for a given α the deviations from Schwarzschild are quite pronounced for small masses, i.e., the EGBd black holes have a much smaller area for the same mass, the EGBd solutions tend toward the Schwarzschild solutions for larger masses.

Fig. 1 also exhibits the relevant components of the stress-energy tensor of a typical static black hole. It reveals that the energy density $\rho = -T_t^t$ is negative in the vicinity of the horizon. This allows these static black holes to circumvent the no-hair theorem and carry scalar hair.

Rotating EGBd black holes.

The inclusion of rotation is essential for astrophysical applications, but also from a theoretical point of view. The domain of existence of rotating EGBd black holes has been explored in Kleihaus, Kunz & Radu (2011), Kleihaus *et al.* (2016) and is exhibited in Fig. 2. This domain of existence is limited by the static EGBd black holes, the Kerr black holes, the extremal rotating EGBd black holes and the set of critical EGBd black holes. The latter arise analogous to the static case, when the radicand of a square root in the horizon expansion vanishes.

On the left of Fig. 2 the scaled area is exhibited versus the scaled angular momentum. It comes as a surprise, that EGBd theory allows for black holes violating the Kerr bound, i.e., possessing $|j| > 1$, although this violation is small. On the right of Fig. 2 for comparison the scaled area is shown versus the scaled GB parameter $\zeta = \alpha/M^2$.

As seen on the left of Fig. 3, the scaled angular momentum reaches its maximum roughly at half the maximal value of the scaled GB coupling, where the critical and the extremal rotating EGBd black holes merge. We note that the extremal rotating EGBd black holes possess a regular metric on the horizon, whereas the dilaton field diverges on the horizon at the poles.

The quadrupole moment of the Kerr black holes is completely fixed by the global charges, $Q = -J^2/M$. Fig. 3 (right), however, shows, that the quadrupole moment of EGBd black holes can considerably differ from the Kerr case. The Kerr values for the scaled moment of inertia are given by $J/(\Omega_H M^3) = 2(1 + \sqrt{1 - j^2})$, thus they are fixed by the value of j . For the EGBd black holes this is no longer the case, where they decrease monotonically from the Kerr value for a fixed j .

Geodesics.

Also the study of the geodesics of these black holes is both of intrinsic interest and of

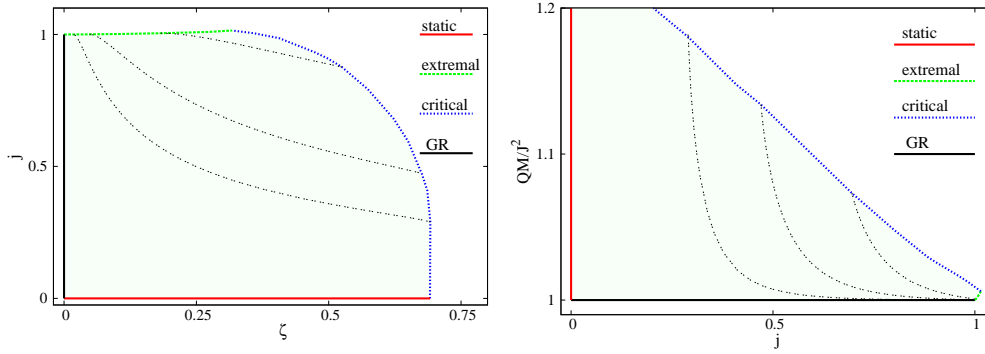


Figure 3. The scaled angular momentum versus the scaled GB coupling constant (left). The scaled quadrupole moment versus the scaled angular momentum (right). Also indicated are the static, the extremal, the critical and the GR black holes.

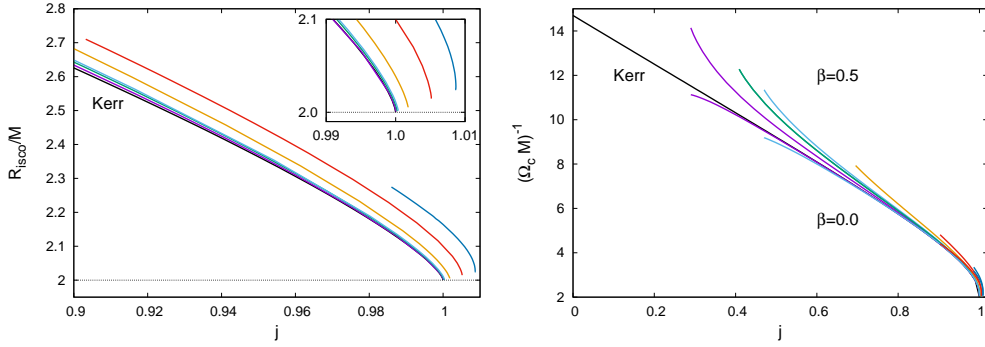


Figure 4. The scaled ISCO radius versus the scaled angular momentum (left). The inverse of the scaled ISCO frequency versus the scaled angular momentum for matter coupling constant $\beta = 0$ and $\beta = 1/2$ (right). The curves correspond to different horizon velocities of the black hole.

astrophysical relevance. The analysis of the geodesics is based on the Lagrangian

$$\mathcal{L} = \frac{1}{2} e^{-2\beta\phi} g_{\mu\nu} \dot{x}^\mu \dot{x}^\nu, \quad (3.2)$$

where β is a coupling constant ($\beta = 1/2$ for string theory). Since the general geodesic equations are not separable (see the discussion in Kleihaus *et al.* (2016), showing the EGBd black holes are of Petrov type I), it is simpler to consider equatorial motion. In particular, we now restrict the analysis to the innermost stable circular orbits (ISCOs) of these black holes.

A perturbative analysis for slow rotation was performed in Pani & Cardoso (2009), while the analysis of the general rotating case was performed in Kleihaus, Kunz & Radu (2011), Kleihaus *et al.* (2016). We exhibit the scaled ISCO radius versus the scaled angular momentum in Fig. 4 (left) for coupling constant $\beta = 1/2$. (The ISCO radius here represents the circumferential radius, not the Boyer-Lindquist coordinate radius.) We note from the figure that the ISCO radius of EGBd black holes exceeds the one of Kerr black holes. Also shown in the figure is the inverse of the scaled ISCO frequency versus the scaled angular momentum (right). As compared to the Kerr case, the frequencies are smaller when $\beta = 1/2$. For $\beta = 0$, however, they are larger.

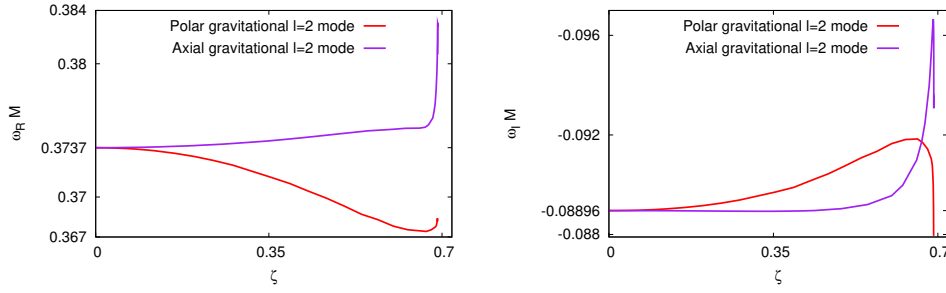


Figure 5. Real (left) and imaginary (right) parts of the gravitational axial and gravitational-led polar $l = 2$ fundamental modes. The Schwarzschild values are recovered at $\zeta = 0$.

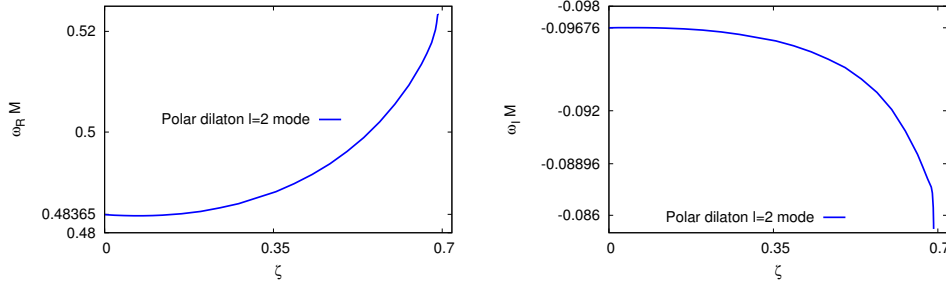


Figure 6. Real (left) and imaginary (right) parts of the scalar-led polar $l = 2$ fundamental modes. The Schwarzschild values are recovered at $\zeta = 0$.

Quasinormal modes and gravitational waves.

When a black hole is perturbed it reacts with the emission of gravitational waves, to settle down again in a stationary state. In an astrophysical setting such perturbations can for instance arise through the infall of a smaller mass, or through the coalescence of black holes. Observation of the latter process was announced earlier this year by the LIGO collaboration Abbott *et al.* (2016). The process consists of three major phases, the inspiral, the merger and the ringdown. We will now briefly address the quasinormal modes of EGBd black holes, relevant for the ringdown phase.

In the following we restrict to the quasinormal modes of static EGBd black holes. The perturbations of the metric and the scalar field are given by

$$g_{ab} = g_{ab}^{(0)} + \varepsilon h_{ab}, \quad \phi = \phi_0(r) + \varepsilon \delta\phi, \quad (3.3)$$

where the subscript zero denotes the unperturbed fields. They can be expanded in terms of spherical harmonics and Fourier transformed, where ω is the Fourier frequency.

To determine the quasinormal modes, we first note, that the modes decouple according to their behavior under parity transformations. The axial modes involve only the metric, while the polar modes involve the dilaton field as well. Imposing physical boundary conditions on the modes, such that the solutions are purely ingoing at the horizon and purely outgoing at infinity, the coupled equations can be solved for the axial and the polar modes (Blázquez-Salcedo *et al.* (2016)).

We exhibit the frequencies of the lowest fundamental axial modes in Fig. 5, where the real part is shown on the left and the imaginary part on the right, versus the scaled GB coupling constant ζ . The Schwarzschild values are recovered at $\zeta = 0$. The deviations

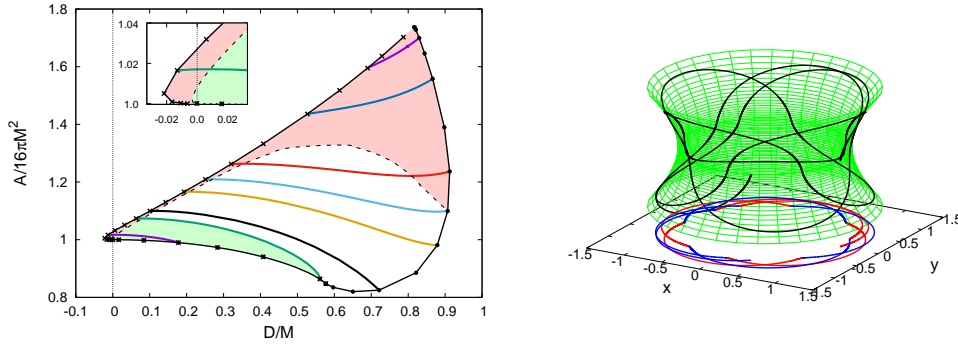


Figure 7. Domain of existence of wormholes in terms of the scaled throat area versus the scaled scalar charge. Wormholes in the lower part of the diagram are expected to be stable (left). Bound orbit of a test particle traveling between the universes (right).

from the Schwarzschild values are small for $\zeta \leq 0.3$, but increase significantly in the vicinity of the critical solution.

For the polar modes we have to distinguish between gravitational-led modes and scalar-led modes. In the limit $\zeta \rightarrow 0$ the gravitational-led EGBd modes reduce to the gravitational modes of the Schwarzschild metric, while the scalar-led EGBd modes reduce to the modes of a test scalar field in the Schwarzschild background. Fig. 5 also shows the frequencies of the lowest gravitational-led EGBd modes, while the scalar-led modes are shown in Fig. 6. As seen in the figures, the deviations from the Schwarzschild modes are somewhat larger for the polar modes.

4. Wormholes

As mentioned in Sec. 2, EGBd theory allows for traversable wormholes without the need for exotic matter, since the quadratic gravitational terms contribute to the effective stress-energy tensor, enabling a violation of the energy conditions (Kanti, Kleihaus & Kunz (2012)). The domain of existence of the resulting static wormholes is exhibited in Fig. 7 (left), where the scaled area of the throat is shown versus the scaled scalar charge. At the left boundary wormholes with a double throat arise, at the lower boundary a transition to black holes is encountered, while at the right boundary solutions with a singularity arise. The lower part of this domain of existence is likely to contain (mode) stable wormholes.

EGBd wormholes possess bound states of test particles, as illustrated in Fig. 7 (right). These may reside in either asymptotically flat universe, but also move between universes. To obtain a low surface gravity at the throat, which is on the order of the gravitational acceleration on the surface of the earth, these wormholes need an astronomical size with a throat radius on the order of 10 - 100 lightyears. Still, smaller EGBd wormholes with higher surface gravity may be considered as potential astrophysical objects, whose observational signatures can be studied.

5. Conclusions and outlook

We have studied the physical properties of black holes in EGBd theory, an astrophysically viable alternate theory of gravity. The coupling constant of the theory has a theoretical bound, and can be constrained by current and future astrophysical observations.

The EGBd black holes differ from their GR counterparts in a number of significant

ways. For instance, they possess a minimal size and mass for a given coupling, their angular momentum can exceed the Kerr bound, and their quadrupole moment can be far bigger. Also, depending on the coupling to ordinary matter, the radii and frequencies of their ISCOs can change considerably. A general analysis of their geodesics is still missing, but their shadow is currently being analyzed. Here further surprises may arise.

We have also analyzed the quasinormal modes of the static EGBd black holes, leaving the analysis of the rotating black holes as a challenge for the future. This analysis leads to the conclusion, that the static EGBd black holes should be mode stable, since all frequencies (calculated) have a negative imaginary part and thus decay exponentially in time. This is in accordance to the results of an early study Kanti *et al.* (1998) where a semi-analytic method demonstrated the stability of these black holes under linear perturbation. On the other hand, the quasinormal modes with the smallest imaginary part control the late-time dynamics of perturbed black holes.

The constraints on the GB coupling are expected to be improved by future observations with third generation gravitational wave detectors. A simple estimate performed in Blázquez-Salcedo *et al.* (2016) leads to the following upper bound on the GB coupling constant

$$\sqrt{\alpha} \lesssim 11 \left(\frac{50}{\rho} \right)^{1/4} \left(\frac{M}{10M_{\odot}} \right) \text{ km} , \quad (5.1)$$

where ρ is the signal-to-noise ratio in the ringdown waveform. The Einstein telescope may achieve a signal-to-noise ratio $\rho \approx 100$ for an event like GW150914. This would then translate into the bound

$$\sqrt{\alpha} \lesssim 8 \left(\frac{M}{10M_{\odot}} \right) \text{ km} \quad (5.2)$$

and $\zeta \lesssim 0.4$.

References

- Berti, E. *et al.* 2015, *Class. Quant. Grav.* 32, 243001
Moura, F. and Schiappa, R. 2007, *Class. Quant. Grav.* 24, 361
Bertotti, B., Iess, L., and Tortora, P. 2003, *Nature* 425, 374
Cantrell, A. G. *et al.* 2010, *Astrophys. J.* 710, 1127
Yagi, K. 2012, *Phys. Rev. D* 86, 081504
Mignemi, S. and Stewart, N. R. 1993, *Phys. Rev. D* 47, 5259
Kanti, P. *et al.* 1996, *Phys. Rev. D* 54, 5049
Torii, T., Yajima, H. and Maeda, K. i. 1996, *Phys. Rev. D* 55, 739
Pani, P., and Cardoso, V. 2009, *Phys. Rev. D* 79, 084031
Kleihaus, B., Kunz, J. and Radu, E. 2011, *Phys. Rev. Lett.* 106, 151104
Pani, P., Macedo, C. F. B., Crispino, L. C. B. and Cardoso, V. 2011, *Phys. Rev. D* 84, 087501
Ayzenberg, D. and Yunes, N. 2014, *Phys. Rev. D* 90, 044066, E: *Phys. Rev. D* 91, 069905
Kleihaus, B., Kunz, J. and Mojica, S. 2014, *Phys. Rev. D* 90, 061501 (2014)
Maselli, A., Pani, P., Gualtieri, L. and Ferrari, V. 2015, *Phys. Rev. D* 92, 083014 (2015)
Kleihaus, B., Kunz, J., Mojica, S. and Radu, E. 2016, *Phys. Rev. D* 93, 044047
Blázquez-Salcedo, J. L. *et al.* 2016, arXiv:1609.01286 [gr-qc].
Kanti, P., Kleihaus B. and Kunz, J. (2012) *Phys. Rev. Lett.* 107, 271101; *Phys. Rev. D* 85, 044007
Abbott, B. P. *et al.* 2016, *Phys. Rev. Lett.* 116, 061102
Maselli, A. *et al.* 2015, *Astrophys. J.* 801, 115
Kanti, P. *et al.* 1998, *Phys. Rev. D* 57, 6255